Papillofoveal Traction in Macular Hole Formation

The Role of Optical Coherence Tomography

Devinder S. Chauhan, FRCOphth; Richard J. Antcliff, FRCOphth; Poornima A. Rai, FRCOphth; Tom H. Williamson, MD, FRCOphth; John Marshall, PhD

Objectives: To determine the validity of the assumption that optical coherence tomographic scans of macular holes have a discrete linear signal (DLS) that represents a detached posterior vitreous face, and to analyze the DLS in macular hole pathogenesis.

Methods: Optical coherence tomographic scans were taken of 3 situations in which the vitreous conditions were known: (1) dissected intact vitreous, (2) clinically evident Weiss rings, and (3) maculae before and after saccades in eyes without a biomicroscopic posterior vitreous detachment. In addition, 70 eyes of 35 patients with macular holes underwent clinical examination and optical coherence tomographic scanning that passed through the optic disc and the fovea or macular hole.

Results: Spatial properties of the DLS matched those of the posterior vitreous face in the situations examined. Of the 70 eyes, 16 (23%) had a biomicroscopic posterior vitreous detachment, whereas a DLS was demonstrated in 40 (57%). Of the 54 eyes without a biomicroscopic posterior vitreous detachment, 18 (33%) had a DLS attached focally to the optic disc margin and the fovea or macular hole. All 7 of the "can opener" holes examined had a nasally "hinged" central flap, 6 with a focally attached DLS.

Conclusions: The DLS corresponds to the posterior vitreous face. Anteronasal papillofoveal traction may generate some macular holes.

Arch Ophthalmol. 2000;118:32-38

From the Department of Ophthalmology, United Medical Schools of Guy's and St Thomas' (Drs Chauhan, Antcliff, and Marshall), and the Vitreoretinal Service, Department of Ophthalmology, St Thomas' Hospital (Drs Rai and Williamson), London, England.

THERE HAVE BEEN many theories on the pathogenesis of macular holes during the past 150 years.[1] The most widely held group of theories invokes tractional forces at the fovea that are exerted at points of vitreofoveal adhesion. In the normal eye, the adhesion at the vitreoretinal interface is thought to be greatest at the vitreous base, the margins of the optic disc, and the overlying major retinal vessels.[2] The anatomical basis of this adhesion consists of 2 junctional systems.[2] The first, and probably the weaker most commonly, is the widespread insertion of cortical vitreous collagen fibrils into the substance of the inner limiting membrane (ILM).[3] The nature of these bonds is believed to be chemical, as electron microscopy reveals no junctional structures.[2] The second is stronger and consists of interspersed junctions between the ILM and Müller cells. At the fovea, the ILM is known to be thin, but the anatomy of the vitreous, and its attachment to the fovea, is somewhat controversial. In vitro studies have demonstrated the presence of a premacular bursa[4] and discrete zones of vitreofoveal adhesion,[5,6] but these have been difficult to corroborate in vivo.[7,8]

In evaluating the pathological changes within this complex, Johnson and Gass[9,10] have previously discounted the role of the ILM and concentrated on the posterior vitreous. Gass initially proposed that spontaneous contraction of the prefoveolar vitreous cortex was the cause of anterior tractional displacement of the foveal retina to the level of the surrounding retina. This was followed by tangential traction and macular hole formation that could begin either centrally without an operculum or paracentrally with an operculum of full-thickness retina.[9,10] In his reappraisal of this theory, Gass[11] suggested that most macular holes begin as a dehiscence at the umbo and not as a result of a foveolar tear and that eccentric tears in the contracted vitreous cortex bridged around a retinal hole. As a consequence, most prefoveolar opacities previously interpreted as operculi are instead the contracted vitreous cortex or pseudooperculi. The reappraised theory was supported by the biomicroscopic observation that the edges of macular holes did not extend anterior to the plane of the retinal surface, as would be expected if there was an anteroposterior tractional component. Studies[12] up to this point had also failed to show evidence of retinal receptors within prefoveolar opacities.

MATERIALS AND METHODS

To address the first aim, OCT images were acquired of the posterior vitreous face in 3 situations. Two of these involved matching the observed DLS to the known location of the posterior vitreous face. In the third, the observed DLS was matched to the known dynamic behavior of the posterior vitreous face. First, intact human vitreous was dissected from cadaveric eyes and, in the absence of an ILM, imaged using OCT. Second, OCT images were acquired of eyes with a complete PVD with a characteristic Weiss ring. The latter is thought to be the site of previous vitreous cortical attachment to the margin of the optic disc. Third, normal eyes without biomicroscopic PVD and in which a DLS was identified on OCT were scanned before and after saccades. These patients were chosen to determine whether the DLS behaved dynamically like the posterior vitreous face. Although the histological components of the tissue generating this signal could not be confirmed, evidence of movement of this signal relative to the retinal surface was sought.

In the second part of the study, OCT scans were performed on both eyes of patients who were seen with an idiopathic macular hole. Particular attention was paid to the imaging of the DLS, or presumed posterior vitreous face. Its state of attachment was noted at the margins of the optic disc and macular holes and at the center of the fovea of unaffected fellow eyes. All studies were performed with informed consent and institutional review board approval.

OCT IMAGING

Images were acquired using a scanner (Optical Coherence Tomography scanner; Humphrey Instruments, San Leandro, Calif). The false-colored cross-sectional images of retina obtained are dependent on the back scattering of partially coherent light, with white and red representing high signal and black corresponding to low signal. The underlying principles and optics of this instrument have been described elsewhere,[17] together with its image interpretation[18] and clinical use.[19] In summary, using a noncontact system, near infrared light is directed through the pupil. This light is scanned in a linear manner, taking approximately 0.9 seconds to acquire information, independent of its length and angular orientation. The image information is stored digitally. The device has an internal fixation light visible to the patient but not on the operator's viewing screen. A second light, generated by a helium-neon (HeNe) laser, is seen on the viewing screen and can be moved under the control of the operator to fall on any given retinal feature. The spatial separation between this light and the ends of the scan line is stored by the computer for each scan orientation. Thus, on subsequent visits, if the operator relocates the HeNe light over the original retinal feature, subsequent scans will be at or close to the same location and orientation.

All clinical examinations and OCT scans were performed following pupillary dilation with 1% guttae (eyedrops) tropicamide and 10% guttae phenylephrine hydrochloride. All clinical OCT scans were acquired using internal fixation alone,[20] and the z-axis location of the scan was manipulated so that the retinal surface was always seen. Any DLS observed was, therefore, within 2 mm of the retinal surface as this is the z-axis limit of the scan image on the commercial OCT instrument. The OCT signal power was always set at its maximum, and the focal plane and polarization of the instrument were adjusted to give the highest possible signal from the DLS.

INVESTIGATION OF VITREOUS HUMOR

Human Vitreous Dissection

Two human cadaveric eyes from a single subject aged 59 years were dissected less than 36 hours post mortem using an established technique.[21] This resulted in an isolated vitreous body sitting on a ring of retina and ciliary body. The absence of an ILM was confirmed by examination with a slitlamp. A suture was passed through this ring to suspend the vitreous body in isotonic sodium chloride solution within a flat-walled, optically clear, glass container. By just resting the equator of the vitreous body on the base of the container and the anterior face against 1 of the container walls, the

Continued on next page

Recent evidence, however, questions the concept of a purely tangential tractional force being the pathogenic mechanism. First, a notable proportion of prefoveolar opacities has been shown to contain neural retinal elements,[13] a finding not wholly compatible with foveal dehiscence as the sole mechanism of full-thickness hole formation. Indeed, Gass[14] recently suggested that the ILM and foveolar Müller cell cones may be present in addition to contracted vitreous as a result, or even consequence, of macular hole formation. Second, the patterns of vitreofoveal relationship seen with retinal imaging techniques such as optical coherence tomography (OCT)[15] and ultrasonography[16] are consistent with an anteroposterior tractional force being applied at the fovea in cases of full-thickness macular holes. Using both of these imaging tools, a discrete linear signal (DLS) can be seen anterior to the macula with focal attachments at the optic disc and fovea. Temporally, the extent of separation varies. This has been interpreted as an incomplete posterior vitreous detachment (PVD) at the posterior pole.[14,15]

This study determines whether the posterior vitreous face generates the DLS seen on OCT, and analyzes the spatial configuration of the DLS in force vectors in macular hole pathogenesis.

RESULTS

INVESTIGATION OF VITREOUS HUMOR

Human Vitreous Dissection

Both vitreous bodies were intact and appeared free of retina and ILM at the posterior surface when viewed with a slitlamp under high magnification using a narrow slit of light. A linear signal corresponding to the posterior vitreous face was seen on scanning both specimens (Figure 1, B). This was confirmed by the observation that gentle agitation of the vitreous body resulted in corresponding movement of this signal. The intensity of this signal, and that from the cortical vitreous, varied with

anteroposterior axis of the vitreous was horizontally oriented. The posterior vitreous was clear of the other walls of the container. This setup was then mounted on a stage with the objective lens of the OCT viewing the anterior vitreous (**Figure 1**, A). An image of the far wall of the container (2 parallel linear signals) was first acquired, and the OCT scanner was then slowly pulled back, while continually scanning, until a signal was acquired corresponding to the posterior vitreous face. The focused image was optimized by adjusting the polarization of the incident light and then stored digitally. The OCT scanner was then pulled back further until another double signal was obtained, corresponding to the anterior wall of the container. This protocol avoided the possibility of recording an image related to the container's walls instead of the vitreous.

Weiss Ring

Three patients with clear ocular media and a well-defined Weiss ring seen on indirect stereobiomicroscopy were imaged with the OCT scanner. Scans were taken passing across a diameter of the ring and extending through the posterior vitreous cortex on each side.

Saccades

Patients selected were those in whom it was possible to identify a DLS less than 2 mm anterior to the macular surface on OCT imaging, without a PVD or retinal disease on biomicroscopy. Of the 516 human subjects previously examined with OCT (excluding those with macular holes), including 87 normal volunteers and 311 subjects older than 65 years, there were only 2 who fulfilled these criteria, and they were recalled for this study. Having established steady fixation on the internal target, an OCT scan was acquired. Once this image was saved, the OCT scanner was left scanning continuously and each subject was asked to look to the left and then rapidly return fixation to the internal target. A second scan was then acquired immediately. This was repeated until at least 2 pairs of scans were of sufficient quality to allow measurement of the distance between the retinal surface and the center of the DLS. Measurements were taken at 9 evenly distributed points across each scan using the commercial OCT software callipers. The presaccadic separations were then compared with the postsaccadic separations using the Wilcoxon signed rank test.

OCT IMAGING OF MACULAR HOLES AND FELLOW EYES

Both eyes of all patients who were seen with macular holes at the Vitreoretinal Service at St Thomas' Hospital, London, England, in the 13 months commencing in February 1997 were enrolled into this study prospectively. All eyes were graded biomicroscopically using a fundus contact lens and oblique slit examination by an experienced vitreoretinal surgeon (T.H.W.) using the classification described by Gass,[11] and OCT scans of all eyes were acquired by 2 of us (D.S.C. and R.J.A.). A PVD was diagnosed only in the presence of a Weiss ring.

Two configurations of OCT scan were performed on all eyes. The first consisted of a series of 3-mm-long radial scans passing through the foveola of uninvolved eyes and the center of macular holes. In the normal eyes, the scan line was moved until it was centered on the thinnest point of the fovea, as determined by viewing the continuously scrolling OCT image. The HeNe spot was then moved to the middle of the corresponding scan line as a reference for the fovea. Eight scans, passing through the HeNe spot, were then acquired at 0°, 30°, 45°, 60°, 90°, 120°, 135°, and 150°. When scanning macular holes, an attempt was made to place the HeNe spot in the center of the hole with the radial series of subsequent scans passing through this point, as previously described. For patients with a macular hole that had a single point of preferred eccentric fixation, this was relatively simple. However, for those patients with more than 1 fixation location, the scan line had to be repositioned before each scan to ensure that it passed through the center of the macular hole. This was determined by viewing the scrolling OCT image and the real-time video fundus image.

The second configuration of scan acquired was linear and passed through the center of the macular hole, or the foveola in unaffected eyes, and the center of the optic disc. The length of this scan varied between eyes.

the polarization of the incident OCT light. The intensity of the optimized linear signal was always too low to be represented as red or white on the standard logarithmic pseudocolor OCT display.

Weiss Ring

For all 3 eyes, all scans passing through the Weiss ring (**Figure 2**) had the same appearance. There was always a DLS corresponding to the posterior vitreous surface on both sides of the Weiss ring and no signal corresponding to the region within the ring. The signal from the Weiss ring itself was always of greater intensity and thicker than that from the posterior vitreous face. The DLS was never red or white.

Saccades

Using the Wilcoxon signed rank test, the DLS was found to have moved relative to the retinal surface significantly in both patients (patient 1, $P = .01$; and patient 2, $P < .001$) (**Figure 3**). The z-axis resolution of OCT is of the order of 20 µm.[15]

OCT IMAGING OF MACULAR HOLES AND FELLOW EYES

Thirty-five patients (27 women and 8 men) were recruited (median age, 71 years; range, 61-81 years). Of the 35 patients, 9 had bilateral macular holes resulting in a total of 44 macular holes seen on biomicroscopy. All stages of hole were identified in this group, and no additional macular holes were diagnosed on OCT imaging.

A DLS was demonstrated unequivocally on OCT scans in 40 (57%) of the 70 eyes, and in an additional 4 (6%) of the 70 eyes was seen on some, but not all, scans (**Table**).

Biomicroscopically, in the absence of a Weiss ring, a posterior vitreous face was identified in only 16 (23%) of the 70 eyes, and in all but 1 of these, there was a prefoveolar opacity identified. In each case, the diameter of

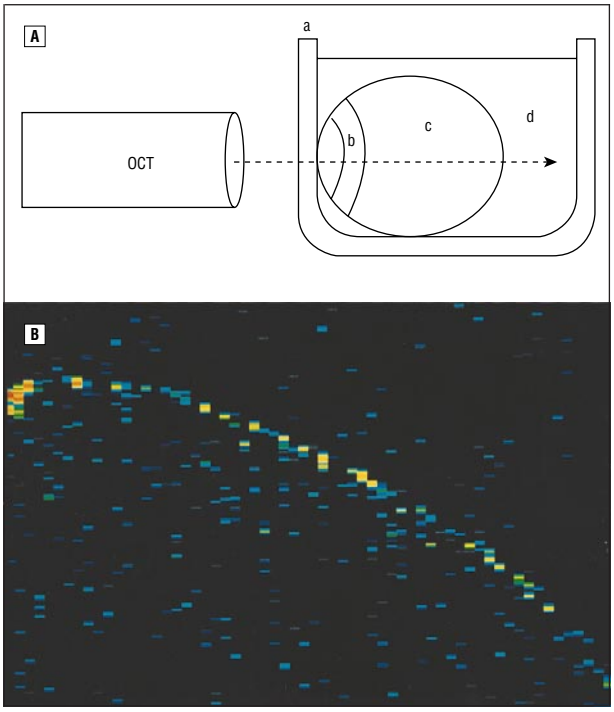

Figure 1. *A, Orientation of the objective lens of the optical coherence tomograph (OCT) relative to the flat-walled, optically clear, glass container (a). The vitreous body (c) and its ring of retina and ciliary body (b) are immersed in isotonic sodium chloride solution (d). B, Optical coherence tomographic scan of dissected human vitreous with a discrete linear signal separating vitreous on the top of the image from isotonic sodium chloride solution on the bottom.*

the prefoveolar opacity was less than that of the macular hole on OCT images. Of the remaining 54 eyes in which there was no biomicroscopically identifiable posterior vitreous face, 18 (33%) of the eyes of 16 patients had a DLS of a specific configuration demonstrated by OCT. In these eyes, the DLS was separate from the macular retinal signal at all points except the margin of the optic disc and the center of the fovea, where it was focally in contact with the retinal surface signal (Table). This pattern was seen with both macular holes and "normal" foveae and was independent of the angular orientation of the scan on the macula (**Figure 4**). A notable subset of eyes in this group consisted of 7 eyes with "can opener" macular holes. In all 7, the orientation of the crescentic hole was such that its apex was temporal and the DLS always spanned from the optic disc margin to the edge of the crescent proximal to the disc (**Figure 5**). The orientation of these macular holes could be confirmed biomicroscopically in 4 cases.

COMMENT

There were 2 notable findings in this study, the first being that the posterior vitreous face contributes to the DLS. Second, the configuration of the DLS was consistent, in some cases, with a partial PVD with persistent attachment to the fovea and optic disc. In none of the present cases was a posterior vitreous face seen on biomicroscopy. The resolution of the DLS configuration into force vectors acting at the fovea suggests the possible existence of a new and prognostically distinct subset of macular holes.

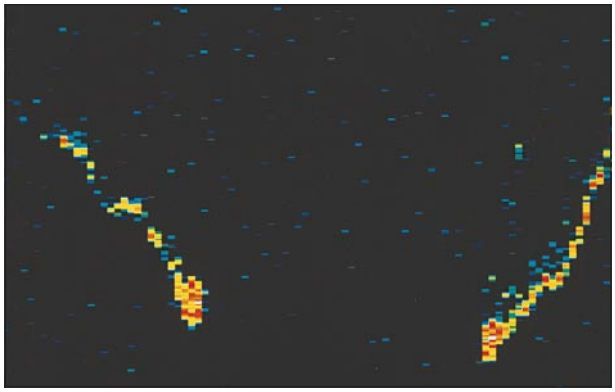

Figure 2. *Two discrete linear signals are seen with increased thickness and intensity medially with a gap between them. These correspond to the posterior vitreous face, the Weiss ring itself, and the gap within it.*

The presence of a DLS on the OCT scan of macular holes has been described previously,[14] when it was assumed that the posterior vitreous face generated the DLS. A DLS was seen in 3 of the 8 cases reported, but in none of these was a single scan taken passing through the macular hole and disc. No conclusions regarding the mechanism of macular hole formation were drawn.

The validity of the assumption that the posterior vitreous face generates the DLS was addressed empirically in the first part of the study. We investigated the nature of the signal itself and its geometry. In the first experiment, eyes were dissected using an established technique for the preparation of vitreous for dark-field slit photography.[19] The immersion of the dissected vitreous in isotonic sodium chloride solution was necessary to maintain the integrity of the tissue architecture but also served to emulate the change in refractive index between a detached posterior vitreous surface and subhyaloid fluid in vivo. Although a surface signal was always present, the intensity of the DLS generated (Figure 1, B) was less than that seen in vivo with a presumed PVD.

High signal, represented by red or white, was seen in the eyes with a Weiss ring but only associated with the ring itself (Figure 2). When analyzing the DLS in vivo, it was not possible to discriminate between the posterior vitreous face and a detached ILM with certainty. This lack of discrimination is due to OCT not having sufficient longitudinal resolution and to the absence of clear differences in the optical properties of the adjacent tissues. Thus, the DLS may have components derived from 1 or both of the ILM and the posterior vitreous face, possibly altered pathologically.[22] This is consistent with the higher-intensity signal seen in these cases compared with the in vitro study. The DLS is unlikely to be generated by the anterior or posterior boundary of a premacular bursa as the patterns of attachment and separation of the DLS to and from the retina, respectively, differ markedly from the anatomical descriptions of these cavities in the literature.[4,5] In the final experiment in this part of the study, the relative movement between the DLS and the retinal surface was statistically highly significant ($P<.01$) and consistent with the known kinetic characteristics of vitreous seen on ultrasonography.[23]

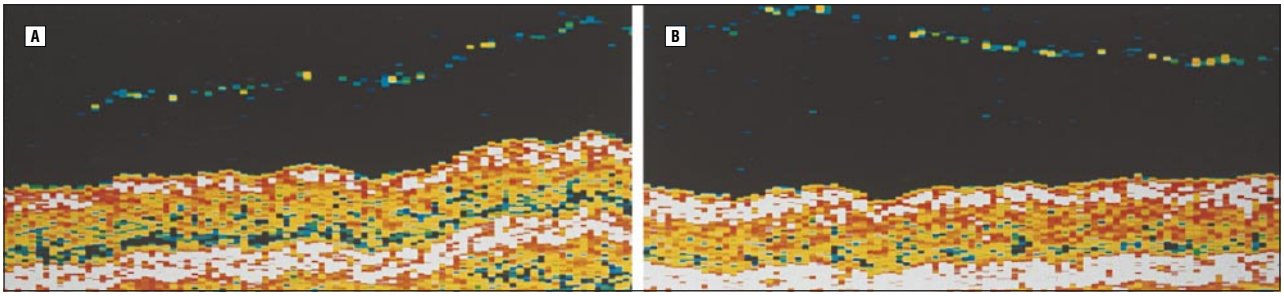

Figure 3. *Optical coherence tomographic scans immediately before (A) and after (B) a single saccadic movement of the eye in a patient without symptoms or signs of posterior vitreous detachment. The discrete linear signal is seen to have moved relative to the retinal surface.*

Results of OCT Examination in Subjects With Macular Holes (MHs)*

	MH Status, No. (%)			
	Eyes		Patients	
	With MHs	Normal Fellows	Bilateral MHs	Unilateral MHs
Total	**44 (100)**	**26 (100)**	9 (100)	26 (100)
DLS with a Weiss ring (classical PVD)	2 (5)	4 (15)	0 (0)	5 (19)
DLS with a prefoveolar opacity and without a Weiss ring	14 (32)	2 (8)	3 (33)	6 (23)
DLS with a focal optic disc and foveal attachments (occult PVD)	11 (25)	7 (27)	0 (0)	12 (46)†
No DLS identified	17 (39)	13 (50)	0 (0)	15 (58)

**Seventy eyes of 35 patients were examined using optical coherence tomography (OCT). Results are given for individual eyes in the first 2 data columns and for both eyes of patients in the 2 columns to the right. For unilateral holes, these data represent the presence of findings in 1 or both eyes. DLS indicates discrete linear signal; PVD, posterior vitreous detachment.*

†*This finding was bilateral in 2 patients.*

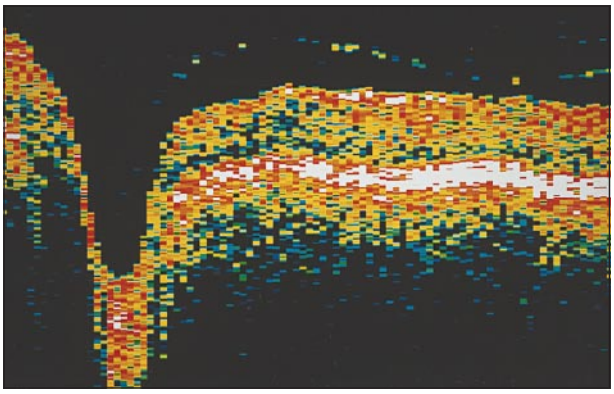

Figure 4. *Optical coherence tomographic scan passing through both the optic disc and fovea. Optical coherence tomographic scan, 7 mm long, of an eye without signs of posterior vitreous detachment, demonstrating the optic disc (left) and a discrete linear signal with a double-convex configuration. The discrete linear signal is attached to the optic disc margin and the fovea.*

The findings described, in static and kinetic situations, confirm that the DLS corresponds to a structure composed, either partly or wholly, of the posterior vitreous face. Thus, the observed pattern of DLS with attachments at the disc margin and the fovea or macular hole probably represents a partial PVD with persistent attachment at the disc margin and fovea. In the present study, this was never observed biomicroscopically and, therefore, might be described as "occult." The subtle vitreous changes in the present patients are unlike the marked changes seen and described in patients with vitreomacular traction syndromes.[24]

The double convex shape of the DLS in such occult PVDs could result from several factors, including system artifact, a posterior vitreous face under tension from anterior forces, and disturbed fluid dynamics causing pooling of fluid in the subhyaloid space. Anterior traction cannot be dismissed but has no morphologic basis on OCT images. In addition, a posterior vitreous face under no tension, or displaced by underlying fluid, would demonstrate differences between horizontal and vertical scans due to gravity. No such differences were observed. The double convex shape could, therefore, be an artifact due to the scanning mechanism of the instrument. A tilting mirror deflecting the scan beam in an arc acquires scans across the x-y plane of the retina. When scanning across the posterior pole, which is concave toward the scanner, the distance between the scanner's objective lens and the retinal surface is roughly constant. The retinal image thus appears flat. However, when scanning a flat surface, the distance between that surface and the objective lens varies, increasing with deviation from normal incidence. The image of this surface thus appears falsely convex. It is, therefore, likely that, if under tension, the posterior vitreous face between the optic disc and the fovea or macular hole edge in such cases of occult PVD lies in the plane of the chord between the 2 (**Figure 6**).

For any contractile forces to act within the posterior vitreous face, such as those suggested by Gass,[10,11] a specific sequence of events must occur. As only cells can actively contract, their migration and subsequent proliferation must occur in the first instance, followed by anchorage and contraction.[25] Candidates for such cells include Müller cells,[14] retinal pigment epithelial cells, fibroblasts, neuroglia, and macrophages.[23] In the presence of an occult PVD, tractional forces within the pos-

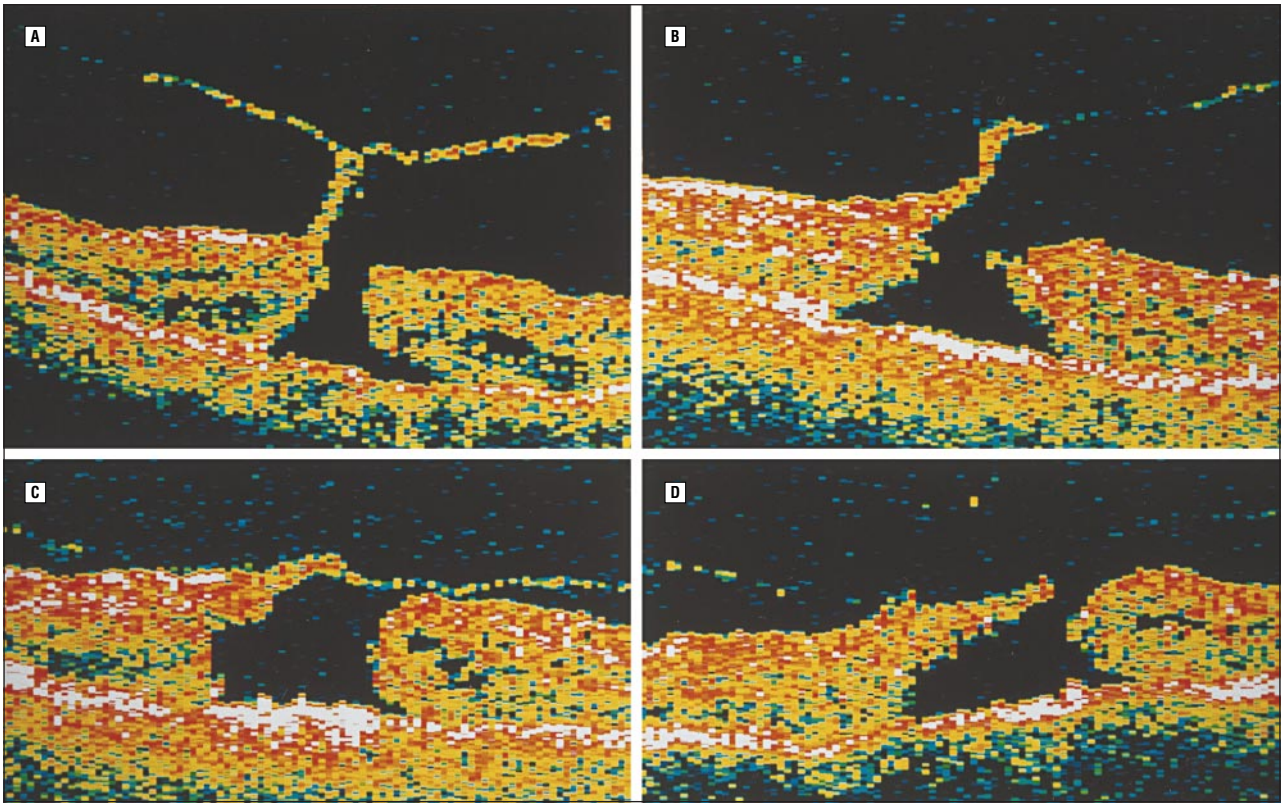

Figure 5. *Optical coherence tomographic scans of 4 of the 7 "can opener" Gass stage 2, macular holes, all of which had a central flap that was "hinged" nasally with a distinct linear signal attached to its apex. All scans are 3 mm long with the optic disc to the left.*

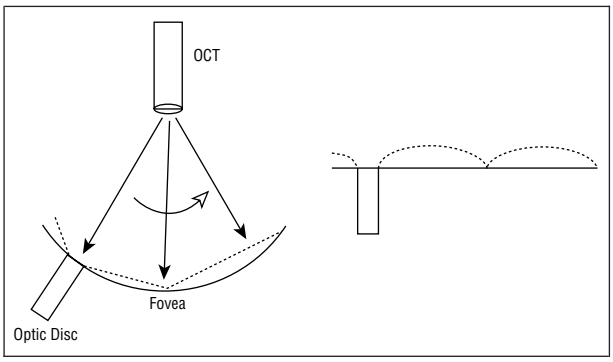

Figure 6. *Explanation of the double-convex configuration of the distinct linear signal. Left, The optical coherence tomographic (OCT) beam (straight arrows) is translated across the posterior pole to obtain a linear scan. This is achieved by a tilting mirror mechanism, resulting in a radial scanning pattern (curved arrow). Right, Most points on the concave retinal surface are equidistant from the OCT, thus appearing to be flat on the image obtained. Those on a partially detached posterior vitreous face (dotted black line) are not, resulting in an artifactual convexity.*

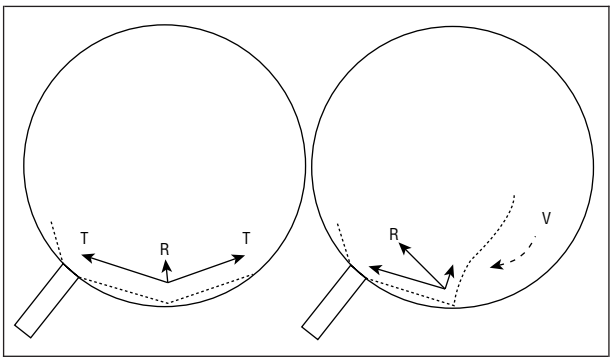

Figure 7. *Simple vector analysis of vitreofoveal tractional forces. Left, Tractional forces (T) within an "occult" partially detached posterior vitreous face (dotted line) may be resolved into an anteriorly directed vector (solid arrows, R), with arrow lengths representing relative magnitude of force. Right, The magnitude and direction of the anteriorly directed vector change with progressive temporal vitreous detachment and the bulk movement of the vitreous (dashed arrow, V). The resultant effect is a significant anteronasally directed (papillofoveal) tractional force.*

terior vitreous face would have a tangential and an anteroposterior component. Temporal to the fovea, the posterior vitreous face in such cases tends to detach further than nasally, retaining a rectilinear signal on B-scan ultrasonography.[15]

The spatial geometry of the proposed vectors is summarized in **Figure 7**. As the 2 sites of firm vitreoretinal adherence are at the disc and fovea, the direct force applied to the fovea would have an anteronasal direction. From simple trigonometry, the anteroposterior component of contraction within the posterior vitreous face would then be 14% of the component acting tangentially along the surface of the retina. This assumes an average eye with an internal equatorial scleral diameter of 24 mm and a disc-foveola distance of 3.4 mm[26] (Figure 7, left). The progressive temporal detachment of the posterior vitreous face and bulk movement of the vitreous generated by saccadic eye movement may be resolved into further anteronasal vectors (Figure 7, right). This proposed mechanism is strongly supported by the observation that all 7 of the eyes in our series with can opener macular holes had a central flap that was "hinged" na-

sally, and 6 had a DLS passing from the temporal edge of the flap to the optic disc margin (Figure 5). Such macular holes are thus probably true rhegmatogenous macular tears. Even before the vitreous detaches from the disc, the predominant direction of pull may be anteronasal and some foveal tissue may be avulsed to form a "true" operculum. The, albeit weak, vitreoretinal attachment temporally would prevent a notable nasal displacement of this tissue. The proportion of patients in this study with occult PVD (46% [16/35])) in either eye is similar to the proportion with prefoveolar opacities previously shown to contain foveal elements.[13] Although this has not been demonstrated herein, it may be that patients with this pattern of occult PVD are those that lose neural retinal tissue to form true operculi.

The discrepancy between the proportion of eyes in which a DLS was identified in any OCT scan (57% [40/70]) and that in which the posterior vitreous face was seen biomicroscopically (23% [16/70]) is probably due to the low-reflectance posterior vitreous face being in close proximity to the high-reflectance retinal surface. The signal from the former is swamped by glare from the latter for the human observer's eye. Indeed, in all but 1 of the eyes in which the posterior vitreous face was observed at the slitlamp, there was a prefoveolar opacity present that may have provided a visual cue for the localization of the posterior vitreous face. In this study, we did not attempt to produce an image of the posterior vitreous without the retinal surface being visible on the scan. As the maximum z-axis dimension of an OCT scan is 2 mm, only a posterior vitreous face within 2 mm of the retinal surface could be identified in the absence of a Weiss ring. This may have led to an underdetection of PVDs. This study consists of high-resolution observations at a single point of macular holes at various stages. Further longitudinal studies are in progress.

In summary, we hypothesize that there is a subgroup of patients with macular holes in whom there is an abnormal, occult form of PVD. In such patients, there is an abnormally persistent attachment of the vitreous to the optic disc margin and fovea, resulting in papillofoveal tractional forces with an anteronasal vector. Full progression in these eyes may lead to the formation of a rhegmatogenous full-thickness macular hole with a true operculum, while earlier vitreofoveal detachment may lead to either the abortion of a macular hole or the development of an arrested macular hole.

It is, therefore, possible that the presence of occult PVD with persistent vitreofoveal attachment is an important prognostic factor. It may be a risk factor indicating poor visual prognosis resulting from the avulsion of foveal tissue. Furthermore, it may well indicate the development of problems in the fellow eye. This study has demonstrated that OCT may be of use in the classification and consequent management of macular holes.

Accepted for publication August 17, 1999.

We thank Anthony H. Chignell, FRCS, FRCOphth, for his invaluable input and encouragement; and Timothy J. ffytche, LVO, FRCOphth, and the Lady Anne Allerton Research Fund, London, England, for their support.

Reprints: Devinder S. Chauhan, FRCOphth, Department of Ophthalmology, St Thomas Campus, United Medical Schools of Guy's and St Thomas', Lambeth Palace Road, London SE1 7EH, England (e-mail: chauhands@aol.com).

REFERENCES

1. Ho AC, Guyer DG, Fine SL. Macular hole. *Surv Ophthalmol.* 1998;42:393-416.
2. Hogan H, Alvarado JA, Weddell JE. *Histology of the Human Eye: An Atlas and Textbook.* Philadelphia, Pa: WB Saunders Co; 1971:393-522.
3. Sebag J. Age-related differences in the human vitreoretinal interface. *Arch Ophthalmol.* 1991;109:966-971.
4. Worst JGF. Cisternal systems of the fully developed vitreous body in the young adult. *Trans Ophthalmol Soc U K.* 1977;97:550-554.
5. Kishi S, Shimuzu K. Posterior precortical vitreous pocket. *Arch Ophthalmol.* 1990;108:979-982.
6. Kishi S, Demaria C, Shimuzu K. Vitreous cortical remnants at the fovea after spontaneous vitreous detachment. *Int Ophthalmol.* 1986;9:253-260.
7. Kiryu J, Ogura Y, Shahidi M, et al. Enhanced visualization of vitreoretinal interface by laser biomicroscopy. *Ophthalmology.* 1993;100:1040-1043.
8. Kakehashi A, Schepens CL, Trempe CL. Vitreomacular observations, I: vitreomacular adhesion and hole in the premacular hyaloid. *Ophthalmology.* 1994;101:1515-1521.
9. Johnson RN, Gass JD. Idiopathic macular holes: observations, stages of formation and implications for surgical intervention. *Ophthalmology.* 1988;95:917-924.
10. Gass JDM. Idiopathic senile macular hole: its early stages and pathogenesis. *Arch Ophthalmol.* 1988;106:629-639.
11. Gass JDM. Reappraisal of biomicroscopic classification of stages of development of a macular hole. *Am J Ophthalmol.* 1995;119:752-759.
12. Smiddy WE, Michels RG, de Bustros S, et al. Histopathology of tissue removed during vitrectomy for impending macular holes. *Am J Ophthalmol.* 1989;108:360-364.
13. Ezra E, Munro PM, Charteris DG, et al. Macular hole opercula: ultrastructural features and clinicopathological correlation. *Arch Ophthalmol.* 1997;115:1381-1387.
14. Gass JDM. Müller cell cone, an overlooked part of the anatomy of the fovea centralis: hypotheses concerning its role in the pathogenesis of macular hole and foveomacular retinoschisis. *Arch Ophthalmol.* 1999;117:821-823.
15. Hee MR, Puliafito CA, Wong C, et al. Optical coherence tomography of macular holes. *Ophthalmology.* 1995;102:748-756.
16. Johnson MW, VanNewkirk MR, Meyer KA. Perifoveal cortical vitreous separation initiates idiopathic macular hole formation [abstract]. *Invest Ophthalmol Vis Sci.* 1998;39(suppl):690.
17. Huang D, Swanson EA, Lin CP, et al. Optical coherence tomography. *Science.* 1991;254:1178-1181.
18. Chauhan DS, Marshall J. The interpretation of optical coherence tomography images of the retina. *Invest Ophthalmol Vis Sci.* 1999;40:2332-2342.
19. Hee MR, Izatt JA, Swanson EA, et al. Optical coherence tomography of the human retina. *Arch Ophthalmol.* 1995;113:325-332.
20. Schuman JS, Pedut-Kloizman T, Hertzmark E, et al. Reproducibility of nerve fibre layer thickness measurements using optical coherence tomography. *Ophthalmology.* 1996;103:1889-1898.
21. Sebag J, Balasz EA. Human virteous fibres and vireoretinal disease. *Eye.* 1985;104:123-128.
22. Grierson I, Mazure A, Hogg P, et al. Non-vascular vitreoretinopathy: the cells and the cellular basis of contraction. *Eye.* 1996;10(pt 6):671-684.
23. Coleman DJ, Lizzi FL, Jack RL. *Ultrasonography of the Eye and Orbit.* Philadelphia, Pa: Lea & Febiger; 1977.
24. Jaffe NS. Vitreous traction at the posterior pole of the fundus due to alterations in the vitreous posterior. *Trans Am Acad Ophthalmol Otolaryngol.* 1967;71:642-651.
25. Grierson I, Joseph J, Miller M, Day JE. Wound repair: the fibroblast and the inhibition of scar formation. *Eye.* 1988;2:135-148.
26. Straatsma BR, Landers M, Kreiger AE. Topography of the human adult retina. *UCLA Forum Med Sci.* 1969;8:379-410.